CHEMICAL ENGINEERING TRANSACTIONS
VOL. 97, 2022
A publication of AIDIC
The Italian Association of Chemical Engineering
Online at www.cetjournal.it
Guest Editors: Jeng Shiun Lim, Nor Alafiza Yunus, Jiří Jaromír Klemeš
Copyright © 2022, AIDIC Servizi S.r.l.
ISBN 978-88-95608-96-9; **ISSN** 2283-9216
DOI: 10.3303/CET2297003

Thermodynamic and Kinetic Analysis of CH_4/C_3H_8 Hydrates for Hydrate-based Gas Separation

Hai Son Truong-Lam[a,*], Ju Dong Lee[b]

[a]Faculty of Chemistry, University of Science, Vietnam National University, Ho Chi Minh City, Viet Nam
[b]Offshore Plant Resources R&D Center, Korea Institute of Industrial Technology, Busan, Republic of Korea
tlshai@hcmus.edu.vn

Gas hydrates have recently attracted attention due to their potential applications in important not only gas separation/recovery but also the related transportation/storage technologies. In this study, hydrate-based gas separation from CH_4/C_3H_8 gas mixture investigated and evaluated. The phase equilibrium condition of which was predicted using the CSMGem software. Hydrate formation from CH_4/C_3H_8 gas mixture 9.5 % C_3H_8 at 3.7 MPa and 275.15 K was also investigated to determine the separation efficiency of CH_4. During hydrate formation, the vapor phase was analyzed by in situ Raman spectroscopy and double-checked by gas chromatography. The Raman data also revealed the structure of the gas hydrate and the time-dependent encapsulation of guest molecules. The experimental results demonstrated that highly concentrated CH_4 can be effectively separated from natural gas hydrates; they will be very useful for methane separation/recovery from natural gas.

1. Introduction

Natural gas assessed the best replacement and environmentally friendly energy source (Tang et al., 2018). It is a mixture of hydrocarbon gases; in particular, it contains predominantly methane and small amounts of other gases, such as ethane, and propane (Schicks and Luzi-Helbing, 2013). The expansion in research exploring natural gas hydrates due to the world's energy demand. (Tang et al., 2018). Clathrates hydrates (gas hydrates) are nonstoichiometric crystalline compounds consisting of water and hydrate molecules (such as natural gas) (Cho, 2019). They generally require high operating pressures and low temperatures to be stable. However, natural gas hydrates can pose a threat to any oil or gas production system as hydrates can plug off a flow line during the production operations (Daraboina et al., 2015), leading to pressure build-up, pipeline rupture, and eventual serious production losses. Therefore, the development method for the determination of the vapor compositions of natural gas hydrate is important for energy recovery and related transportation/storage technologies.

To date, gas chromatography (GC) and infrared absorption spectroscopy (IR) have been used to analyze the natural gas composition. Both analytical methods have their intrinsic limitations; for example, IR cannot detect a sample that contains a large of water; therefore, it does not meet the detection requirements for determining the methane content in natural gas hydrates (Sharma et al., 2016). As for GC, it is destructive and consuming, and it requires a carrier gas (Gao et al., 2019). Unlike these methods, Raman spectroscopy is not affected by water molecules due to their small cross-section (Hédoux, 2016), it has a fast detection speed (analysis period within 1 min) and high sensitivity. For these reasons, Raman spectroscopy has broad applicability in the real-time monitoring of methane during the formation of natural gas hydrates.

In the present study, CH_4/C_3H_8 gas mixture (C_3H_8 9.5 mol%) was selected as the representative natural gas. CH_4/C_3H_8 mixtures may form structure I (sI) or structure II (sII) hydrates depending on the CH_4 concentration in the feed gas, and structure II hydrates are formed when the initial C_3H_8 concentration exceeds 8 mol% (Uchida et al., 2003). The hydrate formation of this mixture at 275.15 K and 3.7 MPa has also investigated the separation efficiency of CH_4. During hydrate formation, the vapor phase was analyzed by GC and in-situ Raman spectroscopy. The Raman data also revealed the structure of the gas hydrate and the time-dependent encapsulation of the guest molecules. The experimental results demonstrated that highly concentrated CH_4 can

Paper Received: 5 May 2022; Revised: 27 July 2022; Accepted: 10 August 2022
Please cite this article as: Truong-Lam H.S., Lee J.D., 2022, Thermodynamic and Kinetic Analysis of CH4/C3H8 Hydrates for Hydrate-based Gas Separation, Chemical Engineering Transactions, 97, 13-18 DOI:10.3303/CET2297003

be effectively separated from natural gas. The novelty of this paper is to investigate and evaluate the thermodynamic and kinetic of CH_4/C_3H_8 gas mixture for hydrate-based gas separation. In particular, this study provides useful information for separating methane gas from natural gas composed of various components.

2. Experimental

2.1 Materials and instruments

Pure methane (> 99.9 %), propane (> 99.9 %), and a methane/propane gas mixture (90.5 % CH_4 and 9.5 % C_3H_8) were supplied by PS Chem Co., Ltd. (South Korea). The experimental equipment (Figure 1) has been described in previous study (Truong-Lam et al., 2020).

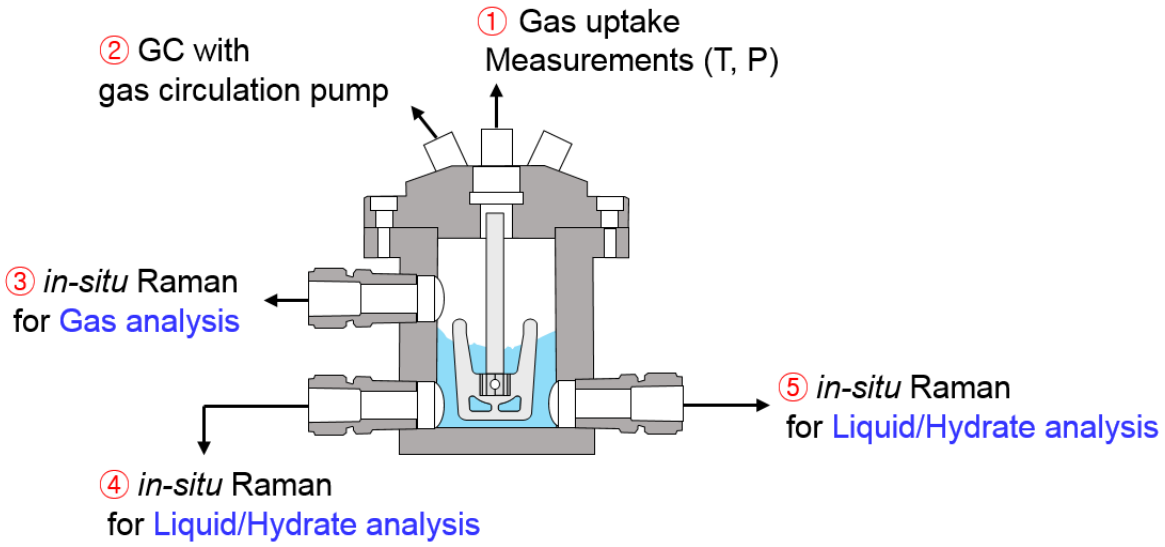

Figure 1: Hydrate reactor layout for gas hydrate formation (GC: gas chromatography; T: temperature, and P: pressure)

2.2 GC conditions

A gas chromatography (GC) model 7890A from Agilent Hewlett Packard, USA equipped with Thermal Conductivity Detector (TCD) and Flame Ionization Detector (FID) system used for the determination of the CH_4, C_3H_8 concentration in the gas mixture. For introducing the gas sample into the GC system, an injection pump (Model 2HM, Eldex, USA) and a six-port switching valve with a 5 µL sampling loop were used to ensure a consistent sample flow. The optimized analytical conditions for GC-TCD and GC-FID methods presented in Table 1.

Table 1: Operating conditions of gas chromatography (GC) system, along with those of its thermal conductivity detector (TCD) and flame ionization detector (FID)

Injection	Injection volume	5 µL
	Temperature	200 ºC
	Column	Molecular sieve 13X, packed column stainless steel, 60/80 Mesh
GC separation	Total flow	30 mL/min
	Column flow	2.0 mL/min
	Temperature program	80 ºC (3 min) (rate of 20 ºC/min) → 180 ºC (1 min)
	Temperature	250 ºC
TCD detection	Flow gas reference	30 mL/min
	Flow makeup	5 mL/min
	Temperature	250 ºC
FID detection	Flow hydrogen	40 mL/min
	Flow air	400 mL/min

2.3 In-situ Raman spectroscopic analysis

A multichannel Raman spectrometer (Lambda Ray Co. Ltd, South Korea) equipped with a laser source of 532 nm having an incident laser power of 100 mW used for the experiments; its spectral range and resolution were 834 – 3810 cm^{-1} and 1 cm^{-1},. Each Raman spectrum was the average of three accumulations for all the experimental conditions, each of which measured over 10 s of spectral integration time. Thus, the Raman spectra were collected every 30 s.

3. Results and discussion

3.1 Vapor phase of the CH_4/C_3H_8 gas mixture

Figure 2 compares the chromatograms of the CH_4/C_3H_8 gas mixture obtained under optimum analytical conditions using the thermal conductivity detector (TCD) and the flame ionization detector (FID). Each gas component was well separated and detected under the given gas chromatography operating conditions.

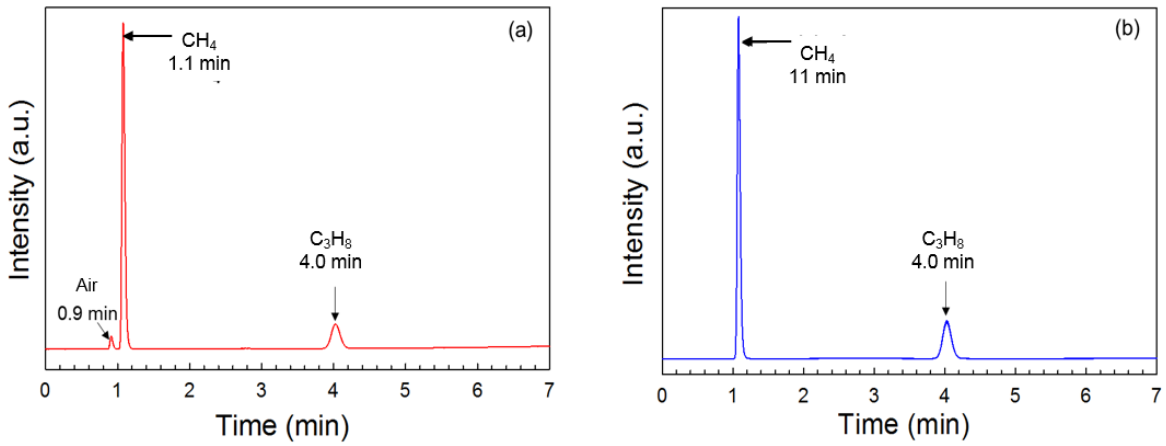

Figure 2: Gas chromatograms of the CH_4/C_3H_8 mixture measured by (a) a thermal conductivity detector and (b) a flame ionization detector, along with their retention times

The Raman spectrum of CH_4 showed a major peak at 2,917 cm^{-1} corresponding to the symmetric stretching of the C-H bonds, while the Raman spectrum of C_3H_8 exhibited two peaks at 874 and 2,886 cm^{-1} attributed to C-C and C-H bonds. The Raman peak positions are consistent with those reported in a previous study (Truong-Lam et al., 2020). Raman spectra and GC chromatograms of CH_4/C_3H_8 gas mixture were acquired at a pressure range of 0.2 to 0.5 MPa and at room temperature (298.15 K). Based on the Placzek's polarizability theory of Raman scattering (White, 2010), CH_4 content in the binary mixture gas was calculated as the ratio between the areas of C-H peak of CH_4 and C-C peak of C_3H_8, which were selected for this purpose because they were the most intense signals (Figure 3). The details of the quantitative analysis of the Raman spectra can be found in previous reports (Truong-Lam et al., 2020).

The GC and Raman spectroscopy techniques were compared by investigating their linearity and accuracy. The linearity of both methods for different gas mixtures was determined by analyzing three replicates at each value of pressure. The mole fractions of the individual gases were calculated according to the Pitzer correlation equation and were plotted against the ratio Raman peak intensity ratio and the peak area chromatogram of each component. A detailed calculation method of Pitzer correlation was provided in our previous papers (Truong-Lam et al., 2020). The linearity results were statistically evaluated for both the GC and Raman spectroscopy techniques. The accuracy refers to the closeness of agreement between these analytical methods with a standard deviation being < 0.2 % (Table 2). The results indicated that both techniques could achieve good linearity and determine the vapor phase composition of CH_4/C_3H_8 gas mixtures.

The method detection limits (MDLs) and method quantitation limits (MQLs) of in situ Raman spectroscopy and GC methods were determined based on signal-to-noise (S/N) of 3 and 10. In particular, the MDLs and MQLs of the Raman spectroscopy method for CH_4 and C_3H_8 were derived from the peak positions of 2,917 cm^{-1} and 2,886 cm^{-1} in the spectrum of a blank sample (i.e., air gas); for the GC method, they were estimated according to the areas of a blank sample chromatogram at the retention time of CH_4 (1.1 min) and C_3H_8 (4.0 min). Besides, to verify the accuracy of these analytical methods, some additional experiments were conducted with the constant temperature (298.15 K) and pressure values ranging from 0.2 to 0.5 MPa. The composition calculations for the vapor phase of CH_4 and C_3H_8 are described in detail in previous studies (Truong-Lam et al., 2020). The

experimental MDLs, MQLs results, along with a comparison of the methane percentages in the vapor phase (Table 2), provide a remarkable basis for the development of a method to determine the gas phase in gas mixtures, which useful for energy recovery and related transport/storage technologies.

Table 2: Method detection limits (MDLs) and method quantification (MQLs) of the Raman spectroscopy and two gas chromatography (GC) techniques (i.e., with a flame ionization detector (FID) and a thermal conductivity (TCD) for methane and its percentages in the vapor phase of a CH_4/C_3H_8 gas mixture.

Pressure (MPa)	In-situ Raman spectrometer			GC-FID			GC-TCD		
	CH_4 (%)	MDLs (mg/L)	MQLs (mg/L)	CH_4 (%)	MDLs (mg/L)	MQLs (mg/L)	CH_4 (%)	MDLs (mg/L)	MQLs (mg/L)
0.2	90.45			90.54			90.65		
0.3	90.44	98.24	327.47	90.62	2.3	7.7	90.46	2.5	8.3
0.4	90.46			90.35			90.50		
0.5	90.43			90.39			90.27		

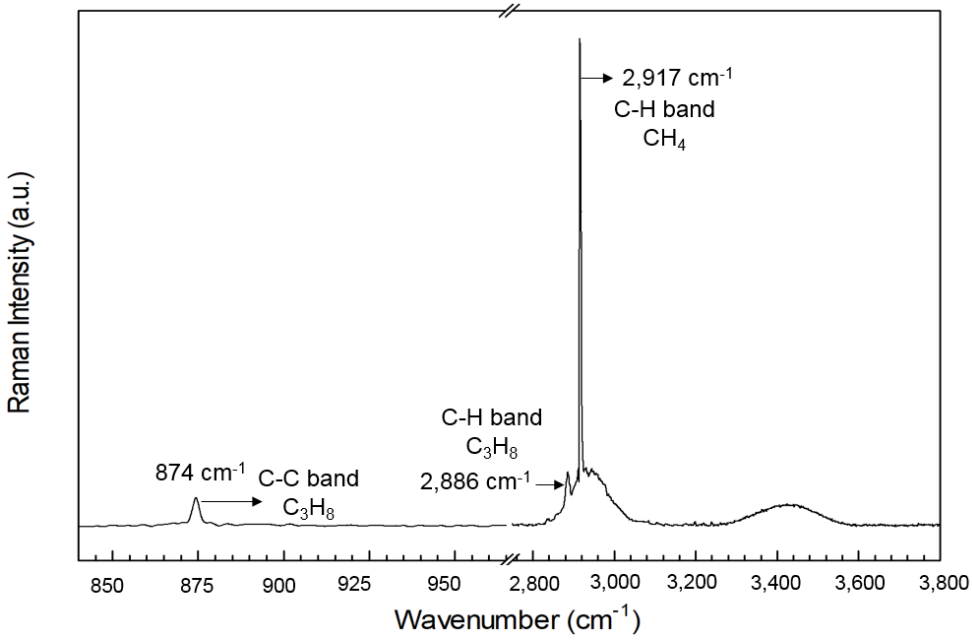

Figure 3: Raman spectrum of CH_4/C_3H_8 gas mixture

3.2 Thermodynamic and dynamic experiments on CH_4/C_3H_8 hydrate formation

To determine the hydrate phase equilibrium (hydrate (H) – liquid water (L_w) – vapor (V)) of CH_4, C_3H_8, and CH_4/C_3H_8 mixture in pure water, the CSMGem software was utilized; the data were calculated in the temperature range of 273.15 – 278.15 K (Figure 4). The Pitzer correlation used to determine the number of moles of mixed gas consumed. Details of these calculations can be found in previous study (Truong-Lam et al., 2021). The equilibrium pressure of hydrate former directly related to the hydrate structure. Structure I hydrate (CH_4) requires higher pressure as compared to CH_4/C_3H_8 hydrates which are structure II hydrates, consistent with the results obtained by Truong-Lam et al. The phase equilibrium data in Figure 4 used to determine the condition of hydrate formation, the experiment carried out at 3.7 MPa, and 275.15 K.

Figure 5 illustrates Raman spectra associated with CH_4/C_3H_8 hydrate formation at 3.7 MPa, 275.15 K. One Raman spectrometer used for the vapor phase analysis and another for investigating the hydrate lattice. The C–H and C-C bonds of C_3H_8 in the gas phase exhibited signals at 2,886 and 887 cm^{-1}, while two peaks observed at 2,870 and 2,878 cm^{-1} were attributed to the C–H stretching of the C_3H_8 molecules in the large cage of sII. The CH_4 molecules showed three characteristic peaks associated with C–H stretching in the vapor phase, and the large and small cages of sII, 2,917, 2,904, and 2,914 cm^{-1}. The vapor phase tended to become enriched in CH_4 (2,917 cm^{-1}) during hydrate formation (Figure 5 (a)). After 60 min, the intensity Raman signal at 887 cm^{-1} and 2,887 cm^{-1} of C_3H_8 gradually decreased to near zero in the end of the experiment. These results could be useful for further studying methane gas separation/recovery processes.

The intensities of both the CH_4 and C_3H_8 hydrate peaks increased as the hydrate formation proceeded (Figure 5(b)), consistently with previous results (Truong-Lam et al., 2020). Their positions did not change when increasing the CH_4 concentration in the vapor phase. The results revealed the formation of sII CH_4/C_3H_8 hydrates and the presence of C_3H_8 in large cages of sII, whereas CH_4 could enter all the available cages (large and small cages of sII hydrates). These observations differ from some previous findings (Kumar et al., 2019). Kwak et al. (2018) reported shifting of the CH_4/C_3H_8 hydrate structure when the propane concentration in the vapor phase is below 8 %. This difference was probably due to the initial pressure conditions, which did not lead to the formation of structure I hydrates in the present study. These results will play an important role in natural gas transportation/storage and its extraction/collection from existing hydrate reserves

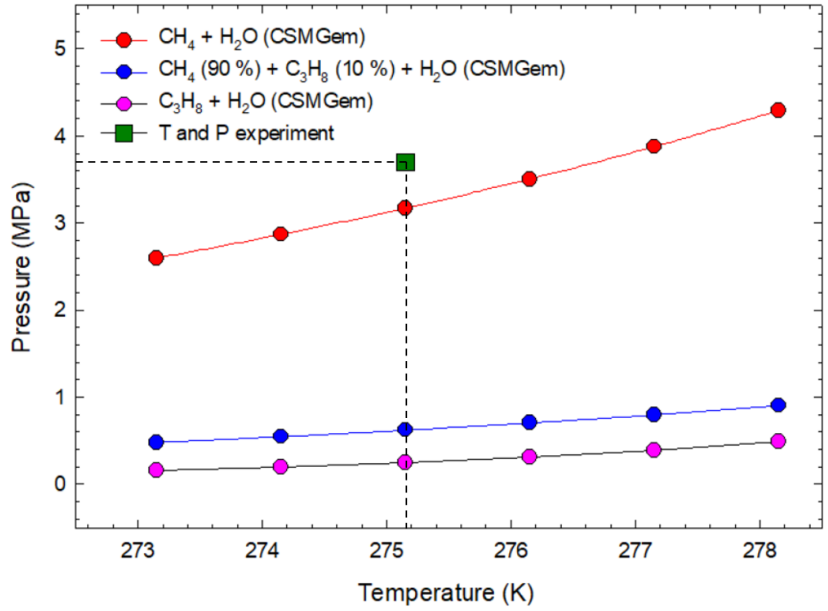

Figure 4: Phase equilibrium condition of CH_4, C_3H_8 and CH_4 (90.5 %)/C_3H_8 (9.5 %) mixture

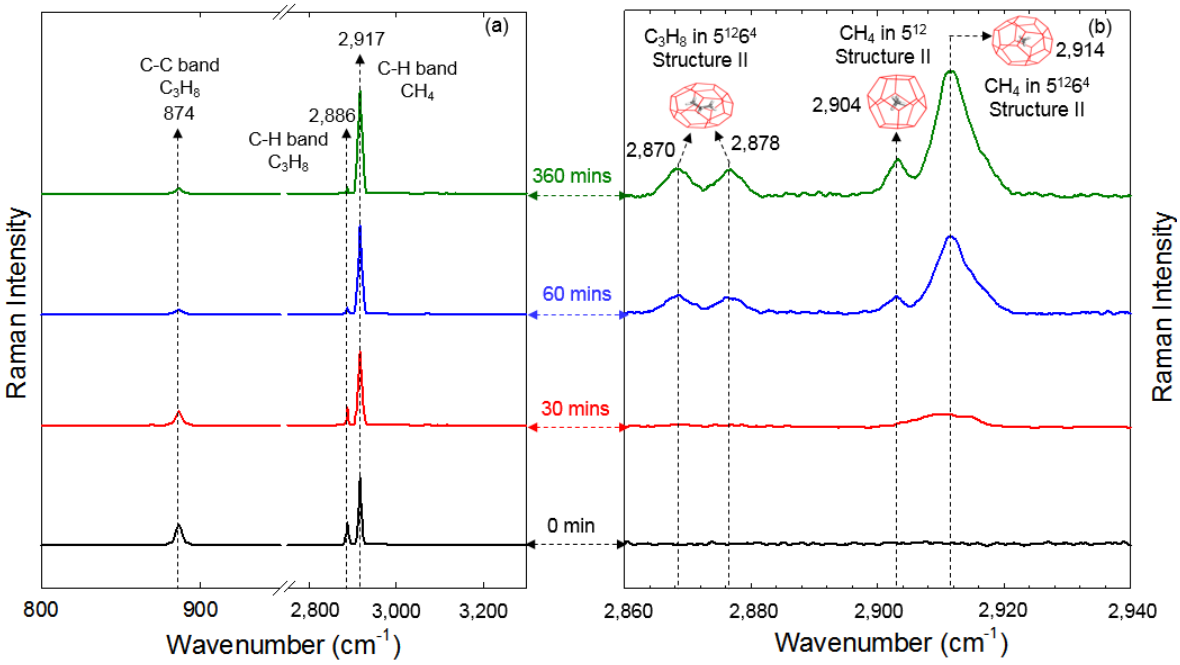

Figure 5: In-situ Raman spectra showing the hydrate formation in a CH_4/C_3H_8 gas mixture at 3.7 MPa and 275.15 K. (a) vapor and (b) hydrate phase analyses.

4. Conclusion

The formation of CH_4/C_3H_8 hydrate from a CH_4/C_3H_8 gas mixture (9.5 % C_3H_8 + 90.5 % CH_4) for application in hydrate-based gas separation investigated from a thermodynamic and kinetic point of view. The in-situ Raman spectroscopy results revealed that the C_3H_8 molecules occupied only the large cage of structure II hydrates, while the CH_4 ones could form both the large and small cages of structure II hydrates. During the kinetic experiments on the CH_4/C_3H_8 hydrate formation, the vapor composition was determined through in situ Raman spectroscopy and the results were consistent with those obtained by GC. The vapor phase in the reactor was almost pure CH_4 by the end of the hydrate formation process. Further studies will be conducted on other gas mixtures of particular interest in the field of natural gas hydrates

Acknowledgments

This research is funded by the University of Science, VNU-HCM under grant number T2022-20.

References

Buldakov M.A., Korolev B.V., Matrosov I.I., Petrov D.V., Tikhomirov A.A., 2013, Raman gas analyzer for determining the composition of natural gas, Journal of Applied Spectroscopy, 80(1), 124–128.

Cho S., Hai T.L.S., Lee J.D., 2019, In-situ Raman and kinetic study on the methane hydrate formation and decomposition, Energy Procedia, 158, 5615–5621.

Daraboina N., Pachitsas S., Von Solms N., 2015, Natural gas hydrate formation and inhibition in gas/crude oil/aqueous systems, Fuel, 148, 186–190.

Gao Y., Dai L.K., Zhu H.D., Chen Y.L., Zhou L., 2019, Quantitative analysis of main components of natural gas based on Raman spectroscopy, Chinese Journal of Analytical Chemistry, 47(1), 67–76.

Hédoux A., 2016, Recent developments in the Raman and infrared investigations of amorphous pharmaceuticals and protein formulations: A review, Advanced Drug Delivery Reviews, 100, 133–146.

Kumar A., Veluswamy H.P., Linga P., Kumar R., 2019, Molecular level investigations and stability analysis of mixed methane-tetrahydrofuran hydrates: Implications to energy storage, Fuel, 236, 1505–1511.

Kwak G.H., Lee K.H., Hong S.Y., Seo S.D., Lee J.D., Lee B.R., Sum A.K., 2018, Phase behavior and Raman spectroscopic analysis for CH_4 and CH_4/C_3H_8 hydrates formed from NaCl Brine and monoethylene glycol mixtures, Journal of Chemical and Engineering Data, 63(6), 2179–2184.

Schicks J.M., Luzi-Helbing M., 2013, Cage occupancy and structural changes during hydrate formation from initial stages to resulting hydrate phase, Spectrochimica Acta - Part A: Molecular and Biomolecular Spectroscopy, 115, 528–536.

Sharma R., Poonacha S., Bekal A., Vartak S., Weling A., Tilak V., Mitra C., 2016, Raman analyzer for sensitive natural gas composition analysis, Optical Engineering, 55 (10), 104103.

Tang C., Zhou X., Li D., Zhao X., Liang D., 2018, In situ Raman investigation on mixed CH_4-C_3H_8 hydrate dissociation in the presence of polyvinylpyrrolidone, Fuel, 214, 505–511.

Truong-Lam H.S., Kim S., Seo S.D., Jeon C., Lee J.D., 2020, Water purifying by gas hydrate: Potential applications to desalination and wastewater treatments, Chemical Engineering Transactions, 78, 67–72.

Truong-Lam H.S., Lee S., Jeon C., Seo S., Kang K.C., Lee J.D., 2021, Effects of salinity on hydrate phase equilibrium and kinetics of SF_6, HFC134a, and their mixture, Journal of Chemical and Engineering Data, 66(5), 2295–2302.

Truong-Lam H.S., Seo S.D., Jeon C., Lee J.D., 2021, Dynamic analysis of growth of ice and hydrate crystals by in situ Raman and their significance in freezing desalination, Crystal Growth & Design, 21(11), 6512–6522.

Truong-Lam H.S., Seo S.D., Kim S., Seo Y., Lee J.D., 2020, In situ Raman study of the formation and dissociation kinetics of methane and methane/propane hydrates, Energy and Fuels, 34(5), 6288–6297.

Uchida T., Takeya S., Wilson L.D., Tulk C.A., Ripmeester J.A., Nagao J., Ebinuma T., Narita H., 2003, Measurements of physical properties of gas hydrates and in situ observations of formation and decomposition processes via Raman spectroscopy and X-ray diffraction, Canadian Journal of Physics, 81(1–2), 351–357.

White S., 2010, Qualitative and quantitative analysis of CO_2 and CH_4 dissolved in water and seawater using laser Raman spectroscopy, Applied Spectroscopy, 64(7), 819–827.